

Interpreting Vibrational Sum-Frequency Spectra of Sulfur Dioxide at the Air/Water Interface: A Comprehensive Molecular Dynamics Study

Marcel Baer,[†] Christopher J. Mundy,^{*,‡} Tsun-Mei Chang,[§] Fu-Ming Tao,[⊥] and Liem X. Dang^{*,‡}

Lehrstuhl für Theoretische Chemie, Ruhr-Universität Bochum, 44780 Bochum, Germany, Chemical and Materials Sciences Division, Pacific Northwest National Laboratory, Richland, Washington 99352, Department of Chemistry, University of Wisconsin–Parkside, Kenosha, Wisconsin 53141, and Department of Chemistry & Biochemistry, California State University, Fullerton, California 92603

Received: January 12, 2010; Revised Manuscript Received: March 30, 2010

We investigated the solvation and spectroscopic properties of SO₂ at the air/water interface using molecular simulation. Molecular interactions from both Kohn–Sham (KS) density functional theory (DFT) and classical polarizable models were used to understand the properties of SO₂:(H₂O)_x complexes in the vicinity of the air/water interface. The KS-DFT was included to allow comparisons with vibrational sum-frequency spectroscopy through the identification of surface SO₂:(H₂O)_x complexes. Using our simulation results, we were able to develop a much more detailed picture of the surface structure of SO₂ consistent with spectroscopic data obtained by Richmond and co-workers (*J. Am. Chem. Soc.* **2005**, 127, 16806). We also found many similarities and differences between the two interaction potentials, including a noticeable weakness of the classical potential model in reproducing the asymmetric hydrogen bonding of water with SO₂ due to its inability to account for SO₂ resonance structures.

I. Introduction

There is an active area of research surrounding the existence and composition of SO₂:(H₂O)_x complexes in the aqueous interfacial region. These are important for understanding SO₂ solvation in aqueous droplets, which is a precursor for acid rain. As a result, the nature of SO₂–H₂O interactions at the aqueous interfaces is of prime importance in many fields, including areas as diverse as atmospheric chemistry and environmental science. SO₂ itself is a major pollutant, and therefore, its interaction with water has received considerable attention in the past. Donaldson and co-workers led the first major experimental effort on this subject by investigating SO₂ adsorption to water using second-harmonic generation back in the early 1990's.¹ Their work provided the first experimental evidence for the existence of a surface-bound state of partially hydrated SO₂. This observation is consistent with our prediction using a potential of mean force approach described in this paper. In addition, a contribution by Devlin and co-workers via a combined spectroscopy and computation study of the ionization of SO₂ on ice surfaces concluded that there was a substantial ionization of SO₂ at low temperatures.² Furthermore, there are contributions by Ewing and co-workers investigating the formation of the SO₂–clathrate systems using spectroscopy.³

Richmond and co-workers recently studied the solvation properties of SO₂ at the air/water interface using vibrational sum-frequency spectroscopy (VSFS).^{4,5} Their study conjectured that there exists a weak SO₂:H₂O complex at the interface prior to SO₂ reaction and dissolution into the aqueous boundary layer. Through a vibrational fingerprint, they were able to assign this

feature to a particular structural moiety at the uppermost surface layer of the air/water interface. In this study, we investigate the interaction of SO₂ with water at the air/water interface using molecular simulations based on both empirical polarizable classical potentials and Kohn–Sham (KS)⁶ density functional theory (DFT).⁷ We used constrained molecular dynamics to sample the motion of the SO₂ as a function of the distance from the interface to determine the corresponding potential of mean force (PMF). One of our main goals is to make a direct comparison to the measured data, and we also discuss ways to improve the agreement between molecular simulations and observed data, including new interpretations of the aqueous surfaces.

II. Computational Method

The Dang–Chang (DC) polarizable model was used to describe water–water interactions.⁸ A new polarizable potential model for SO₂ was developed to accurately describe SO₂–H₂O interactions. The potential parameters were optimized to accurately reproduce high-level ab initio interaction energies (MP2/6-31+G(d,p)) with respect to distance for the SO₂:H₂O complex (i.e., –3.8 kcal/mol and 3.0 Å).⁹ The details can be found in the Supporting Information (S1). Both SO₂ and water were modeled using empirical potentials that explicitly included polarizability. It should be pointed out that although the classical model reproduces the interaction energy as a function of the S–O_w (here the subscript “w” denotes the oxygen on the water) distance, the geometry of the SO₂:H₂O complex is not preserved in the familiar “sandwich” geometry (which is shown as an inset in Supporting Information S1).^{10–13} However, in a previous study, it was shown that barriers of rotations from the global minimum to other local minima are very low;¹⁰ thus, we believe this deficiency in the empirical model will not lead to serious errors for the S–O_w interaction. More detailed comparisons of the classical and KS-DFT interaction potentials and how these differences affect the liquid structure will be made later in the

* Corresponding authors. E-mail: chris.mundy@pnl.gov, liem.dang@pnl.gov.

[†] Ruhr-Universität Bochum.

[‡] Pacific Northwest National Laboratory.

[§] University of Wisconsin–Parkside.

[⊥] California State University.

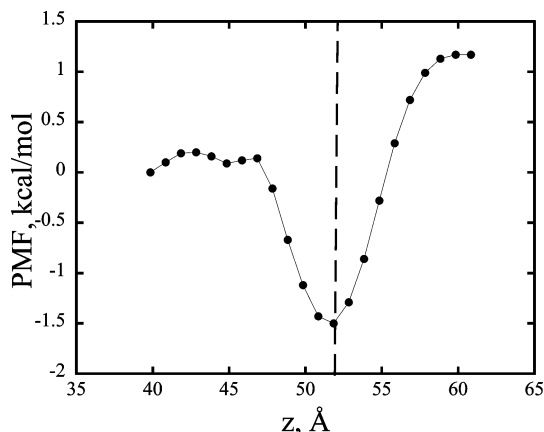


Figure 1. Computed potential of mean force of transferring a SO_2 molecule across the air/water interface at 300 K using the constrain mean force approach.

manuscript. Molecular dynamics (MD) simulations utilizing the KS-DFT were performed on a classically pre-equilibrated system of 215 water molecules and a single SO_2 molecule in a slab geometry with dimensions of $15.0 \times 15.0 \times 71.44 \text{ Å}^3$ using the QUICKSTEP¹⁴ method as implemented in the CP2K code (<http://cp2k.berlios.de>). Details of the calculation are given in the Supporting Information (S2). The analysis of the KS-DFT runs were performed on multiple replicas (>4) of 10 ps production trajectories for both the bulk and interfacial region.

III. Results and Discussion

To assess the equilibrium solvation behavior of SO_2 , the free energy profile for transporting a SO_2 molecule across the air/water interface was calculated within the classical potential using a constrained molecular dynamics technique. For this study, a system with a slab geometry with 600 water molecules in a $26.3 \times 26.3 \times 76.3 \text{ Å}^3$ simulation cell (with two air/water interfaces formed normal to the z -axis) was employed. The resulting free energy profile for SO_2 as a function of the z -coordinate across the air/water interface computed with the classical models is shown in Figure 1. Our calculated value for the free energy of solvation is $\Delta G = -1.3 (\pm 0.1) \text{ kcal/mol}$, which compares well with the experimental value $\Delta G_{\text{expt}} = -2.0 (\pm 0.3) \text{ kcal/mol}$.¹⁵ Our nonreactive classical polarizable interaction potentials predict that the SO_2 molecule has a large propensity for the air/water interface. In the Supporting Information (S5 Figure 3), we compute the density profile of a SO_2 solution at finite concentration using molecular dynamics simulations, which also further corroborates this result by showing enhanced density at the air–water interface.

The prediction of enhanced interfacial SO_2 concentration is interesting when juxtaposed onto the experimental finding; namely, that one observes a red shift in the water-free OH (i.e., hydrogens pointing toward the air) bond frequency when there is a steady SO_2 gas interacting with the air/water interface.^{4,5} It was also observed that upon removing the SO_2 gas, the spectrum quickly returned to that of the neat air–water interface.^{4,5} The analysis of the VSFS spectra given by Richmond and co-workers suggests that the red shift of the “free” water OH signal is due to hydrogen bonded $\text{SO}_2\text{:H}_2\text{O}$ complexes, the so-called “A” moiety, where a water molecule is hydrogen bonded to SO_2 as a π electron acceptor.^{4,5} They speculated that this proposed arrangement likely takes place above the Gibb’s dividing surface (GDS). Through our simulations, we aim to test this conjecture by examining the structure of the $\text{SO}_2\text{:}(\text{H}_2\text{O})_x$ complex under both bulk and interfacial solvation.

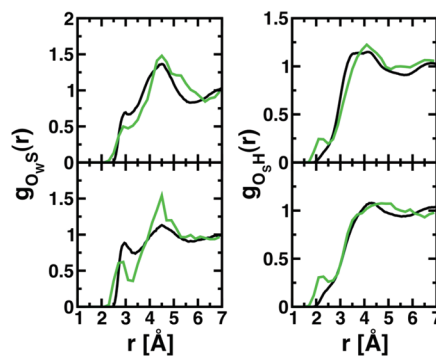


Figure 2. The RDF for conditions of bulk (top) and interfacial (bottom) solvation for the classical (black) and DFT (green) interaction potentials. The interfacial RDFs were scaled to unity at large distances.

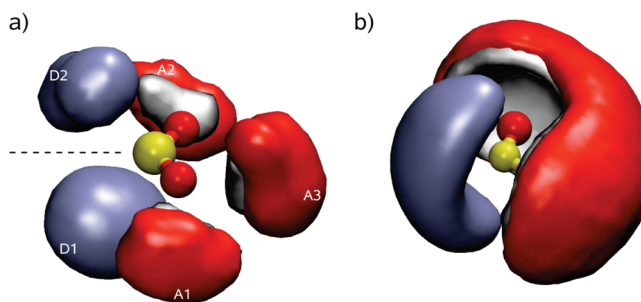


Figure 3. The surface density plots for the DFT (panel a) and the classical (panel b) interaction potentials under bulk solvation conditions. Blue surfaces denote the O_w density; white surfaces, the H density; and red surface, the corresponding O_w . One sees that the classical model is symmetric in the hydrogen bonding (white and red surfaces), whereas the DFT shows three accepting sites (A1–A3), and it is clearly asymmetric. In addition, it is important to note that the donating electrons (D1–D2) of the O_w clearly lie localized on the opposite sides of the mirror plane (dotted line), and this is not the case for the classical model.

To compare the structure between the KS-DFT and classical interaction potentials, the S–O_w radial distribution functions (RDFs) are given in Figure 2. There is reasonable agreement between the two, which is expected, since the SO_2 interaction potential was parametrized to the S–O_w potential energy (see Supporting Information (S1) for details). This is also an indication that although the minimum energy dimer geometry is not recovered with our classical model, some features of the water molecule packing around the sulfur are still reproduced in comparison with KS-DFT. Differences between the two interaction potentials appear in the first solvation shell when one examines the RDF in Figure 3 for the $\text{O}_s\text{–H}$ RDF (the subscript “s” denotes the oxygen that is associated with the water and sulfur). Here, the DFT interaction potential shows significantly more structure, which is likely due to the ability of DFT to effectively capture the resonance structures of SO_2 . The consequence of the resonance structures will be manifest in an asymmetric solvation structure as shown in Figure 3 and in Table 1. Moreover, the ability of the classical potentials to capture this asymmetry will become more important in the vicinity of the air/water interface. This suggests that although the classical interaction potential, which is based on point charges and scalar isotropic polarizability, produces similar average structures, as seen from Figure 2, it is unable to reproduce the $\text{SO}_2\text{:H}_2\text{O}$ resonance structures, which may be important in the hydrogen bonded state of SO_2 .

As was indicated in the experimental investigation, the origin of the observed red shift in the mid-IR region in the presence

TABLE 1: The Interaction States of SO₂ Depicted for the DFT Interaction Potential for the Bulk and Interface Environment^a

S—O _w	O _s -H						
	0/0, %	1/0, %	1/1, %	2/0, %	1/2, %	2/2, %	
0	4.5	5.7	1.9	0.3	0.2	0.0	bulk
	18.4	12.0	0.3	0.4	0.0	0.0	interface
1	7.6	27.0	23.3	5.0	6.1	4.3	bulk
	19.2	25.5	21.6	2.0	0.5	0.0	interface
2	1.0	5.0	6.8	2.0	4.1	0.2	bulk
	0.4	0.0	0.0	0.0	0.0	0.0	interface

^a The column denotes the number of S—O_w interactions, the rows denote the symmetrized hydrogen bonding states of O_s. Special attention should be made to the bold entries. The (0, 1/0) is most closely related to the A type moiety, as denoted by Richmond and co-workers, and the (1, 0/0) most closely resembles the B type moiety in the language of Richmond and co-workers.^{4,5} Both of these populations are enhanced at the interface, but they are not the dominant populations. What is apparent is that the majority of the SO₂ moieties involve the (1, 1/0) or the (1, 1/1) arrangement in agreement with “sandwich” geometry that is seen SO₂ in its cluster hydrated form. In stark contrast, as shown in the Supporting Information, the classical interaction potential does not produce a stable hydrogen bonding SO₂ that can also be observed from the RDFs. Thus, there is no A moiety that can exist within the classical model, and thus, the ensemble of its structures cannot explain the experimentally observed spectral features.

of flowing SO₂ gas may be present in the SO₂:H₂O complexes at the water surface.^{4,5} Since the observed VSFS signal is coming from the first or second layers at the interface, it is likely that the SO₂:H₂O moieties will be microsolvated. We can bring additional insight by simulating the spectra of small microsolvated clusters of SO₂:(H₂O). To this end, we compared the relative energetics of optimized clusters obtained via MP2 and DFT calculations using the same basis set and density cutoff

as was used for the MD simulations; see the Supporting Information (Figure S2) for details.

We can examine the IR spectra through performing MD calculations on SO₂(H₂O)_{*n*}, with *n* = 1, 3, using the KS-DFT interaction potential. The IR spectra were computed with the usual dipole–dipole autocorrelation functions via a standard Wannier analysis.^{16–18} Results for the vibrational spectra of clusters of SO₂(H₂O)_{*n*}, with *n* = 1, 3, are depicted in Figure 4. The salient interpretation of the cluster spectra is that the addition of extra hydrating water molecules shifts the frequencies to the red relative to the free OH oscillator. These results are in good agreement with a previous experimental and theoretical study¹⁹ and are consistent with the VSFS experiments.^{4,5} Interestingly, none of the minimum energy clusters (see the Supporting Information, Figure S2) shows the presence of the so-called A moiety, in which a single water molecule is hydrogen bonded to SO₂ as a π electron acceptor. This is not surprising when we acknowledge that the minimum energy “sandwich” SO₂:H₂O moiety will most likely be preserved.^{10–13} Although it is clear that the experimentally conjectured A and B moieties are not to be taken as exact structural motifs, much can be learned from using these ideas as starting points to interpret the observed spectra.

An explanation of the red shift based on our simulation data can be found in examining two and three water clusters with SO₂ in different orientations to mimic possible structures that may be present at the air–water interface in the presence of SO₂ gas. These configurations are shown in Figure 5. The top and bottom panels in Figure 5 denote clusters of SO₂ with two and three waters, respectively. Each cluster is then reoriented with assigned frequencies corresponding to those of water’s OH oscillator that obey a selection rule consistent with the orientation being perpendicular to the interface. A red shift can be found in the mid-IR for nearly all orientations of the clusters relative to the free OH stretch, as shown in Figure 4.

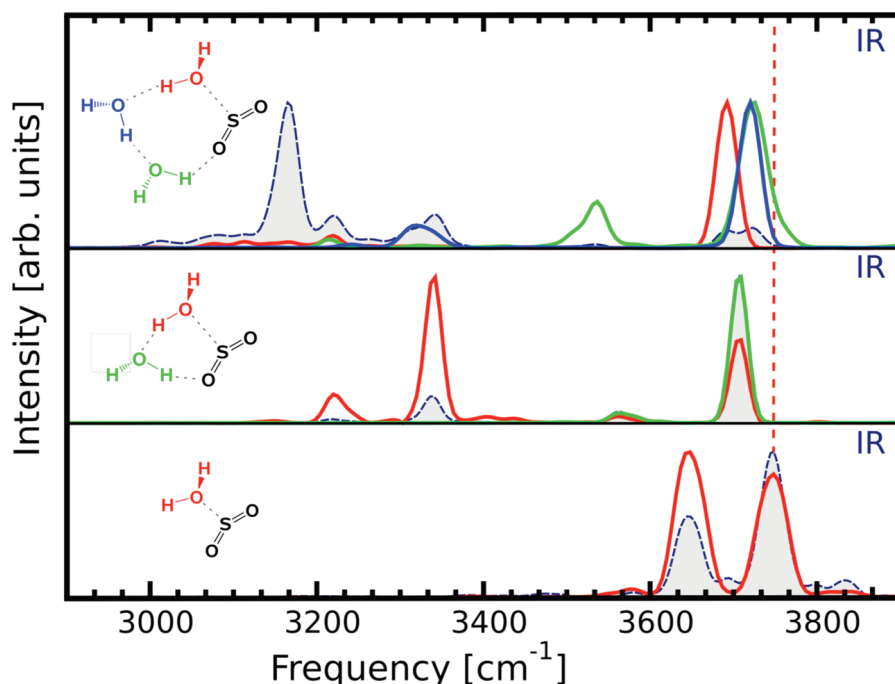


Figure 4. Infrared spectra (IR) of the hydrated SO₂ clusters. The total IR spectrum in each panel is rendered in a solid gray scale. The individual contribution to the IR by the solvating water molecule is denoted in red, green, or blue, corresponding to the schematic cluster on the left-hand side of each panel. It is clear from the IR spectra that hydration produces a relative red shift in the free OH oscillator, given by the vertical red dashed line. This suggests, together with the surface moieties denoted in Figure 6, that these hydrated SO₂ clusters in the vicinity of the GDS are responsible for the observed spectra.

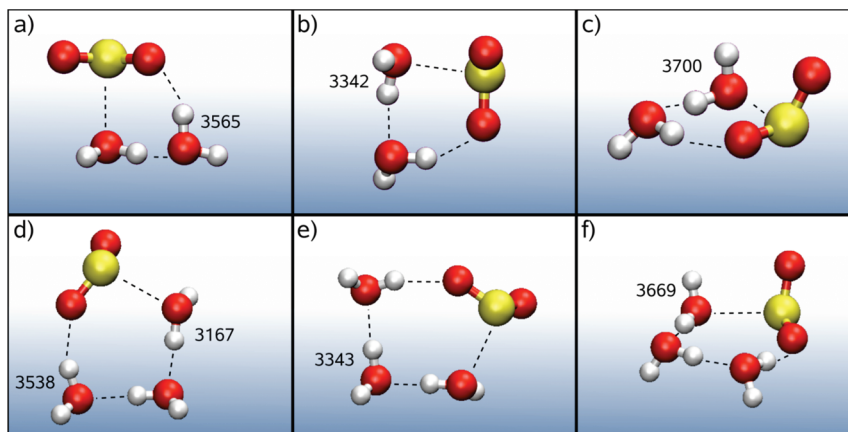


Figure 5. The top and bottom panels denote the hydrated structure of SO_2 with two and three hydrating waters, respectively. Each cluster is then reoriented with assigned frequencies corresponding to those OH oscillators that obey a selection rule consistent with the orientation being perpendicular to the interface being in the plane of the page. It is important to note that these moieties that are represented by the clusters are not arbitrary microstates, but represent the surface populations (1, 0/1). The (1, 0/1) moieties make up 25% of the surface by our calculations in Table 1.

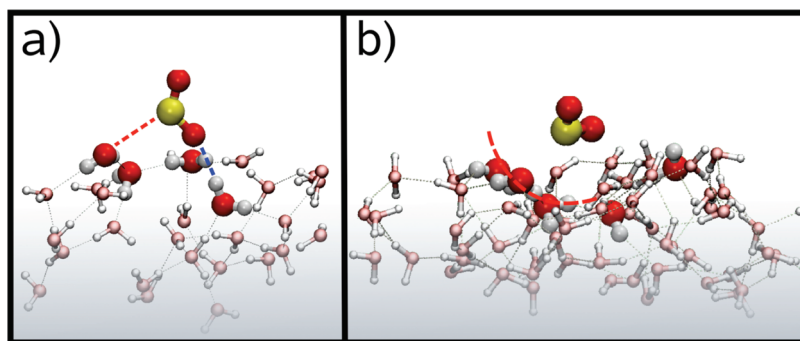


Figure 6. A representative configuration from the surface of the DFT (panel a) and the classical (panel b) simulations are depicted. These configurations were chosen on the basis of the most probable bonding arrangement as computed in Table 1. The red and blue dashed lines in panel A represent the $\text{S}-\text{O}_w$ and the O_s-H (respectively) in the (1, 0/1) configuration. The curved dashed line in panel b shows the oxygen that is involved in the O_w-S interactions based on the classical model. It is clear that both surfaces are modified by the interaction with SO_2 .

To make contact with the cluster studies, we analyzed our surface trajectories by comparing the relative populations of different types of water binding with SO_2 . This was done by determining the number of $\text{S}-\text{O}_w$ bonds (which ranged from 0 to 2) and the number of bonds between each sulfur oxygen (O_s) and the water hydrogens, which could range from 0 to 2 for each O_s . To represent O_s-H hydrogen bonds, we use a nomenclature of a/b , where a represents the number of hydrogen bonds with one SO_2 oxygen, and b the number with the other. For example, the 1/0 state is with one of the O_s 's being involved in a hydrogen bond, and the other O_s , not. The definition of a bond between $\text{S}-\text{O}_w$ was a distance less than 3.5 Å, and the definition of a bond between O_s-H was 2.2 Å. Table 1 shows that for the DFT interaction potential, there is, indeed, asymmetric hydrogen bonding (or one O_s hydrogen bonding more than the other) that occurs with a significant population in the bulk and at the interface. We are also able to identify the populations of the A and B states as postulated from Richmond and co-workers as the (0, 1/0) and (1, 0/0) states, respectively.^{4,5} Both the A and B states are shown to have population enhancements at the interface, but are not the dominant populations. The dominant populations are of the (1, 1/0) and (1, 1/1) forms, which is suggestive of the “sandwich” moiety that is found in our cluster studies.^{10–13} This finding implies that our simplified interpretation of the IR spectra through the hydrated clusters is meaningful. Moreover, it is shown in the Supporting Information (S1), that the classical interaction potential does not capture this important hydrogen bonding state of SO_2 , as can be observed from Figure 2.

Through Table 1, and Figures 2 and 3, we have a reasonable idea of the relevant moieties of SO_2 that are in the vicinity of the air–water interface. Representative configurations from both the classical and DFT interaction potentials are given in Figure 6. At first glance, one observes that the DFT interaction potential yields an $\text{SO}_2:\text{H}_2\text{O}$ complex that resembles the A moiety put forth by Richmond and co-workers.^{4,5} A closer look reveals that the A moiety does not occur in isolation, but in the form of clusters with water, where the “sandwich” structure of the $\text{SO}_2:\text{H}_2\text{O}$ dimer^{10–13} simultaneously exists, as suggested by Table 1. These results are in agreement with the experimentally inferred importance of larger $\text{SO}_2:(\text{H}_2\text{O})_x$ clusters giving rise to the red shift.^{4,5} The configurations from the classical simulations produce a picture in which there is no strong hydrogen bonding of SO_2 to a neighboring water, which is consistent with the computed RDFs. However, it is clear that both interaction potentials produce a picture in which SO_2 modifies the interfacial water structure. We can speculate that this modification could act as an additional source of the observed red shift. This is because the dangling water OH bonds could be forced to rotate into the interfacial plane, producing stronger hydrogen bonds. In the absence of being able to compute the IR spectra of the rigid DC interaction potential, the structure that is put forth in Figure 6 also suggests the presence of nontrivial modification of the hydrogen bond network in the vicinity of SO_2 . However, a more quantitative picture of the precise nature of the structural modification is only afforded through the use of DFT interaction potentials.

IV. Conclusion

In summary, we have used both KS-DFT and classical polarizable interaction potentials to investigate the transport and vibrational spectra of a SO₂ molecule across the air/water interface. The computed free energy profile for the classical potential shows a minimum near the GDS. From this, it is reasonable to conclude that a relatively large concentration of unreacted SO₂ at the air–water interface would alter the surface vibrational spectra, even after the SO₂ gas is shut off.^{4,5} To make contact with experiment, we found that the SO₂:(H₂O)_n, *n* = 2,3 can give rise to the observed red shift in the free OH as well as alter the hydrogen bonding region of the mid-IR (~3400 cm⁻¹). We critically examined the differences between the classical and DFT interaction potentials, and both interaction potentials show agreement in the second solvation shell. However, the ability to describe the resonance structures in the first solvation shell is required. Our data suggests that the red shift in the vibrational spectra when SO₂ gas is flowing could be explained as the SO₂ molecule's inducing ordered SO₂:(H₂O)_x clusters in the vicinity of the interface, giving rise to stronger hydrogen bonds, in agreement with experiment. The polar orientations of interfacial water molecules, their orientations, and “crude” surface IR spectra of the neat water interface have been discussed at length in the literature by one of us.^{20,21} The sampling of the vibrational density of states yields a free OH feature that is significantly more broad than the experimental one due to finite statistics afforded by DFT calculations.^{4,5,20} We believe it would be difficult to assign this red shift on only the basis of the vibrational density of states.

Although it was not necessary to invoke the significant amount of SO₂ adsorption predicted by the classical model as shown in Figure 1 to interpret the experimental spectra, further research is needed to fully understand the contributions of the first solvation shell structure to the free energy of adsorption of SO₂ at the air–water interface. Beyond the analysis of the cluster hydrates of SO₂, our analysis suggests that SO₂ modifies the structure of water above the GDS (see Figure 6). This modification could produce a more ordered hydrogen bonded network, shifting the free OH oscillators at the neat air–water interface inward and thus inducing “stronger” hydrogen bonds. This hypothesis could also be consistent with experimental observations and will be further investigated in a future study.

Acknowledgment. This work was performed at Pacific Northwest National Laboratory (PNNL) and was supported by the Division of Chemical Sciences, Biosciences and Geosciences Office of Basic Energy Sciences, U.S. Department of Energy (DOE). PNNL is operated by Battelle for DOE. C.J.M. thanks I.-F. Will Kuo at Lawrence Livermore National Laboratories for fruitful discussions about the technical details of the DFT

simulations. Calculations were enabled by a 2008–2010 INCITE award to C.J.M. on the CRAY XT4 (using resources of the National Center for Computational Sciences at Oak Ridge National Laboratory (ORNL), which is supported by the Office of Science of the U.S. DOE under Contract No. DE-AC05-00OR22725) and the BlueGene/P at Argonne National Laboratory (resources of the Argonne Leadership Computing Facility at Argonne National Laboratory, which is supported by the Office of Science of the U.S. DOE under Contract No. DE-AC02-06CH11357). C.J.M. also acknowledges the resource NWe located in the Environmental Molecular Sciences Laboratory at PNNL. M.B. gratefully acknowledges partial financial support by Deutsche Forschungsgemeinschaft (DFG) and by Fonds der Chemischen Industrie (FCI) through grants to Dominik Marx (Bochum).

Supporting Information Available: Additional information as noted in text. This material is available free of charge via the Internet at <http://pubs.acs.org>.

References and Notes

- (1) Donaldson, D.; Guest, J.; Goht, M. *J. Phys. Chem.* **1995**, *99*, 9313.
- (2) Jagoda-Cwiklik, B.; Devlin, J.; Buch, V. *Phys. Chem. Chem. Phys.* **2008**, *10*, 4678.
- (3) Zhang, Z.; Ewing, G. *J. Phys. Chem. A* **2004**, *108*, 1681.
- (4) Tarbuck, T. L.; Richmond, G. L. *J. Am. Chem. Soc.* **2005**, *127*, 16806.
- (5) Tarbuck, T. L.; Richmond, G. L. *J. Am. Chem. Soc.* **2006**, *128*, 3256.
- (6) Kohn, W.; Sham, L. *J. Phys. Rev.* **1965**, *140*, 1133.
- (7) Hohenberg, P.; Kohn, W. *Phys. Rev. B* **1964**, *136*, B864.
- (8) Dang, L. X.; Chang, T. M. *J. Chem. Phys.* **1997**, *106*, 8149.
- (9) Bishenden, E.; Donaldson, D. J. *J. Phys. Chem.* **1998**, *102*, 4638.
- (10) Cukras, J.; Sadlej, J. *J. Mol. Struct.: THEOCHEM* **2007**, *819*, 41.
- (11) Matsumura, K.; Lovas, F. J.; Suenram, R. D. *J. Chem. Phys.* **1989**, *91*, 5887.
- (12) Garden, A. L.; Lane, J. R.; Kjaergaard, H. G. *J. Chem. Phys.* **2006**, *125*, 144317.
- (13) Li, W. K.; McKee, M. L. *J. Phys. Chem. A* **1997**, *101*, 9778.
- (14) VandeVondele, J.; Krack, M.; Mohamed, F.; Parrinello, M.; Chassaing, T.; Hutter, J. *Comput. Phys. Commun.* **2005**, *167*, 103.
- (15) Holleman, A. F.; Wiberg, E. *Inorganic Chemistry*; Academic Press: New York, 2001.
- (16) Berghold, G.; Mundy, C. J.; Romero, A. H.; Hutter, J.; Parrinello, M. *Phys. Rev. B* **2000**, *61*, 10040.
- (17) Baer, M.; Mathias, G.; Kuo, I. F. W.; Tobias, D. J.; Mundy, C. J.; Marx, D. *ChemPhysChem* **2008**, *9*, 2703.
- (18) Kimmel, G. A.; Matthiesen, J.; Baer, M.; Mundy, C. J.; Petrik, N. G.; Smith, R. S.; Dohnalek, Z.; Kay, B. D. *J. Am. Chem. Soc.* **2009**, *131*, 12838.
- (19) Hirabayashi, S.; Ito, F.; Yamada, K. M. T. *J. Chem. Phys.* **2006**, *125*, 034508.
- (20) Kuo, I. F. W.; Mundy, C. J. *Science* **2004**, *303*, 658.
- (21) Kuo, I. F. W.; Mundy, C. J.; Eggimann, B. L.; McGrath, M. J.; Siepmann, J. I.; Chen, B.; Vieceli, J.; Tobias, D. J. *J. Phys. Chem. B* **2006**, *110*, 3738.

JP100310S